

## $\text{Sr}_2\text{CrOsO}_6$ : End point of a spin-polarized metal-insulator transition by $5d$ band filling

Y. Krockenberger,<sup>1,2,\*</sup> K. Mogare,<sup>2</sup> M. Reehuis,<sup>2,3</sup> M. Tovar,<sup>3</sup> M. Jansen,<sup>2</sup> G. Vaitheeswaran,<sup>2,4</sup> V. Kanchana,<sup>2,4</sup> F. Bultmark,<sup>5</sup> A. Delin,<sup>4</sup> F. Wilhelm,<sup>6</sup> A. Rogalev,<sup>6</sup> A. Winkler,<sup>1</sup> and L. Alff<sup>1,†</sup>

<sup>1</sup>Darmstadt University of Technology, Petersenstrasse 23, 64287 Darmstadt, Germany

<sup>2</sup>Max-Planck-Institute for Solid State Research, Heisenbergstrasse 1, 70569 Stuttgart, Germany

<sup>3</sup>Hahn-Meitner-Institut (HMI), 14109 Berlin, Germany

<sup>4</sup>Department of Materials Science and Engineering, Royal Institute of Technology (KTH), 10044 Stockholm, Sweden

<sup>5</sup>Department of Physics, University of Uppsala, Box 530, 75121 Uppsala, Sweden

<sup>6</sup>European Synchrotron Radiation Facility (ESRF), 6 Rue Jules Horowitz, Boîte Postale 220, 38043 Grenoble Cedex 9, France

(Received 13 December 2006; published 22 January 2007)

In the search for new spintronic materials with high spin polarization at room temperature, we have synthesized an osmium-based double perovskite with a Curie temperature of 725 K. Our combined experimental results confirm the existence of a sizable induced magnetic moment at the Os site, supported by band-structure calculations, in agreement with a proposed kinetic-energy-driven mechanism of ferrimagnetism in these compounds. The intriguing property of  $\text{Sr}_2\text{CrOsO}_6$  is that it is at the end point of a metal-insulator transition due to  $5d$  band filling and at the same time ferrimagnetism and high-spin polarization are preserved.

DOI: [10.1103/PhysRevB.75.020404](https://doi.org/10.1103/PhysRevB.75.020404)

PACS number(s): 75.50.Pp, 61.12.Ld, 78.20.Fm, 81.05.Zx

A so-called half-metal is a highly desired material for spintronics, as only charge carriers having one of the two possible polarization states contribute to conduction. In the class of ferrimagnetic double perovskites such half-metals are well known—e.g.,  $\text{Sr}_2\text{FeMoO}_6$ .<sup>1</sup> The compound  $\text{Sr}_2\text{CrOsO}_6$  described here is special, as it has a completely filled  $5d t_{2g}$  minority-spin orbital, while the majority-spin channel is still gapped. It is thus at the end point of an ideally fully spin-polarized metal-insulator transition. At the metallic side of this transition we have the half-metallic materials  $\text{Sr}_2\text{CrWO}_6$  (Ref. 2) and  $\text{Sr}_2\text{CrReO}_6$  (Refs. 3 and 4). Within the unique materials class of double perovskites, therefore, one can find high-Curie-temperature ferrimagnets with spin-polarized conductivity ranging over several orders of magnitude from ferrimagnetic metallic to ferrimagnetic insulating *tunable* by electron doping. Note that  $\text{Sr}_2\text{CrOsO}_6$ , where a regular spin-polarized  $5d$  band is shifted below the Fermi level, is fundamentally different from a diluted magnetic semiconductor, where spin-polarized charge carriers derive from impurity states.

While for simple perovskites such as the half-metallic ferromagnetic manganites the Curie temperature  $T_C$  is in the highest case still close to room temperature, half-metallic ferrimagnetic double perovskites can have a considerably higher  $T_C$ .<sup>5</sup> It has been suggested that ferrimagnetism in the double perovskites is kinetic energy driven.<sup>6–8</sup> In short, due to the hybridization of the exchange-split  $3d$  orbitals of  $\text{Fe}^{3+}$  ( $3d^5$ , majority-spin orbitals fully occupied) or  $\text{Cr}^{3+}$  ( $3d^3$ , only  $t_{2g}$  are fully occupied) and the nonmagnetic  $4d/5d$  orbitals of Mo, W, Re, or Os ( $N$  sites), a kinetic energy gain is only possible for the minority-spin carriers. This will lead to a corresponding shift of the bare energy levels at the nonmagnetic site and a strong tendency to half-metallic behavior. This mechanism is operative for the  $\text{Fe}^{3+}$  and  $\text{Cr}^{3+}$  ( $M$  sites) compounds,<sup>2</sup> where all  $3d$  majority-spin states and all  $t_{2g}$  majority-spin states, respectively, are fully occupied and represent localized spins. In agreement with band-structure calculations<sup>1,2,6,9–11</sup> this mechanism is naturally associated

with half-metallic behavior, as the spin-polarized conduction electrons mediate antiferromagnetic order between  $M$  and  $N$  ions and, thus, ferromagnetic order between the  $M$  sites. In addition, this mechanism will lead to an *induced* magnetic moment at the nonmagnetic sites as Mo, W, Re, or Os, in convincing quantitative agreement with recent band-structure calculations. It has been suggested and verified by observation of the corresponding x-ray magnetic circular dichroism (XMCD) that the induced magnetic moment at the nonmagnetic site scales with  $T_C$  of the compound<sup>12–14</sup> or, in other words, the bandwidth in the conducting minority-spin channel scales with the magnetic transition temperature. This behavior has also been confirmed qualitatively by nuclear magnetic resonance (NMR) experiments for FeRe-based double perovskites.<sup>15</sup> Quantitatively, however, Re shows an unusually enhanced induced magnetic moment in the double-perovskite structure, as compared to Mo, W, and Os.

An obvious way to change the band filling is by doping at the alkaline earth site. Substituting, for example,  $\text{Sr}^{2+}$  by  $\text{La}^{3+}$  results in electron doping. For the ferrimagnetic double perovskites it has been shown that increasing the bandwidth by La doping generically increases  $T_C$ .<sup>16,17,19</sup> The increase is substantial—i.e., more than 100 K per one doped electron per unit cell. However, there is an alternative way of doping by using the  $N$  site itself.<sup>20</sup> Within this line of thinking there is a natural explanation why  $\text{Sr}_2\text{CrReO}_6$  was up to now the ferrimagnetic double perovskite with the highest Curie temperature, 635 K.<sup>3</sup> Compared to  $\text{Sr}_2\text{CrWO}_6$  [ $T_C \approx 450\text{--}500$  K (Refs. 2, 18, and 19)] with  $\text{W}^{5+}$  ( $5d^1$ ),  $\text{Sr}_2\text{CrReO}_6$  with  $\text{Re}^{5+}$  ( $5d^2$ ) possesses just one electron more in the minority-spin channel. Therefore, it corresponds to the compound  $\text{LaSrCrWO}_6$ . The increase of  $T_C$  by more than 100 K in both cases [as estimated from the case of  $\text{LaSrFeMoO}_6$  (Ref. 16) and  $\text{LaCaCrWO}_6$  (Ref. 19)] underlines the justification of this comparison. Following this argument,  $\text{Sr}_2\text{CrOsO}_6$  with  $\text{Os}^{5+}$  ( $5d^3$ ) becomes a natural candidate for an ordered ferrimagnetic double perovskite with even higher  $T_C$ . After an early attempt to synthesize this

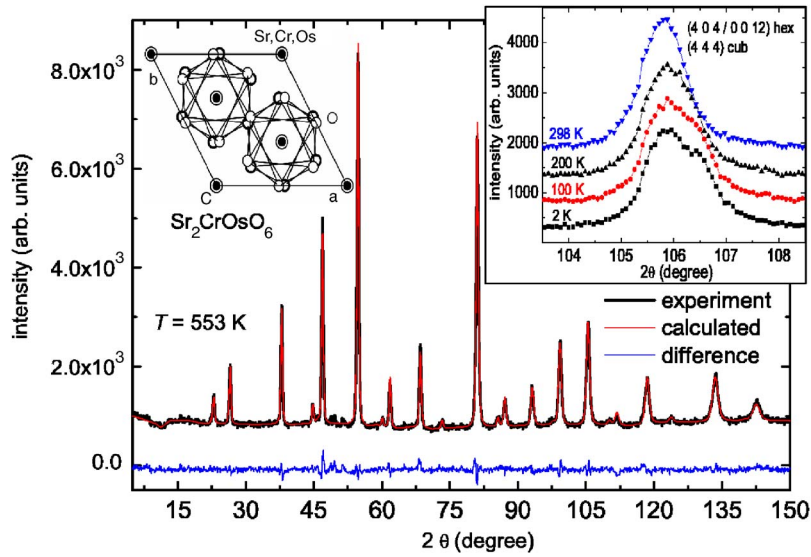


FIG. 1. (Color online) Rietveld refinements of the neutron powder data of  $\text{Sr}_2\text{CrOsO}_6$  taken at 553 K. The observed and calculated diffraction intensities as well as the difference pattern are shown. The upper left inset shows a view along the  $[111]$  direction revealing the rhombohedral structure of the double perovskite. The upper right inset shows the temperature dependence of the  $\text{Sr}_2\text{CrOsO}_6$  (444) diffraction peak (cubic) splitting into a (404) and (0 0 12) peak (hexagonal).

compound, it has been (erroneously) concluded that it is *not* ferromagnetic at room temperature.<sup>21</sup> The CrTa, CrW, CrRe, CrOs series is an ideal system to study the effect of  $5d$  band filling. In order to investigate these ideas we have synthesized phase-pure polycrystalline  $\text{Sr}_2\text{CrOsO}_6$  samples and measured the net magnetization by superconducting quantum interference device (SQUID) magnetometry. The (magnetic)

crystal structure has been extensively studied by neutron scattering and XMCD.

Single-phase polycrystalline samples of  $\text{Sr}_2\text{CrOsO}_6$  have been prepared from stoichiometric amounts of  $\text{SrO}_2$  and  $\text{CrO}_2$  (both Sigma-Aldrich, 99.999%) and Os metal (Chempur 99.99%) at 1273 K in evacuated quartz tubes. The mixture was ground thoroughly, pressed into pellets, and put

TABLE I. Results of the structure refinements of  $\text{Sr}_2\text{CrOsO}_6$ . For the neutron powder data collected at 2 K, 100 K, 200 K, and 298 K the crystal structure was refined in the trigonal space group  $R\bar{3}$ . At the higher temperatures 540 K and 770 K the refinements were carried out in the cubic space group  $Fm\bar{3}m$ . The residuals of the crystal and magnetic structures are defined as  $R_N = \sum ||F_0| - |F_c|| / |F_0|$  and  $R_M = \sum ||I_0| - |I_c|| / |I_0|$ , respectively. For the refinements several parameters were constrained to be equal. In these cases the standard deviation is listed only for one of the equal parameters. As distortion we define  $c / (\sqrt{6}a)$ —i.e., the ratio  $c/a$  normalized to the value of a cubic structure in hexagonal notation ( $\sqrt{6}$ ). See also Ref. 23.

$T$ [K]	2	100	200	298	540	770
Space group	$R\bar{3}$	$R\bar{3}$	$R\bar{3}$	$R\bar{3}$	$Fm\bar{3}m$	$Fm\bar{3}m$
$a$ [Å]	5.5176(3)	5.5170(4)	5.5178(3)	5.5181(6)	7.8243(2)	7.8455(3)
$c$ [Å]	13.4447(14)	13.4540(11)	13.4698(13)	13.4995(13)	7.8243	7.8455
$V$ [Å <sup>3</sup> ]	354.47(4)	354.64(4)	355.16(4)	355.98(8)	479.00(4)	482.90(5)
$c/a$ (hex)	2.4367(4)	2.4386(3)	2.4412(4)	2.4464(8)	$\sqrt{6}$	$\sqrt{6}$
Distortion	0.9948	0.9956	0.9966	0.9988	1	1
$x(\text{O})$	0.3351(13)	0.3351(15)	0.3356(17)	0.335(4)	0.2511(5)	0.2511(5)
$y(\text{O})$	0.1908(7)	0.1900(7)	0.1876(8)	0.1830(14)	0.2511	0.2511
$z(\text{O})$	0.4169(6)	0.4171(7)	0.4171(8)	0.4168(19)	0.2511	0.2511
$z(\text{Sr})$	0.2509(13)	0.2512(15)	0.2510(18)	0.252(4)	0.25	0.25
$B(\text{Sr})$ [Å <sup>2</sup> ]	0.36(4)	0.40(4)	0.48(4)	0.63(4)	1.09(4)	1.47(5)
$B(\text{Cr, Os})$ [Å <sup>2</sup> ]	0.21(2)	0.22(2)	0.25(2)	0.30(3)	0.42(3)	0.51(4)
$B(\text{O})$ [Å <sup>2</sup> ]	0.45(3)	0.47(3)	0.50(3)	0.67(3)	1.41(3)	1.72(4)
$d(\text{Cr-O})$ [Å]	1.947(7)	1.948(8)	1.946(9)	1.949(19)	1.965(4)	1.970(4)
$d(\text{Os-O})$ [Å]	1.957(7)	1.955(8)	1.957(9)	1.956(19)	1.965	1.970
$R_N$	0.039	0.040	0.040	0.037	0.034	0.039
$\mu_{\text{Cr}}$ [ $\mu_B$ ]	2.0(3)	1.9(3)	2.0(3)	1.9(2)	1.8(2)	0
$\mu_{\text{Os}}$ [ $\mu_B$ ]	-0.7(3)	-0.6(3)	-0.3(2)	-0.1(2)	-0.05	0
$R_M$	0.070	0.082	0.065	0.078	0.103	—

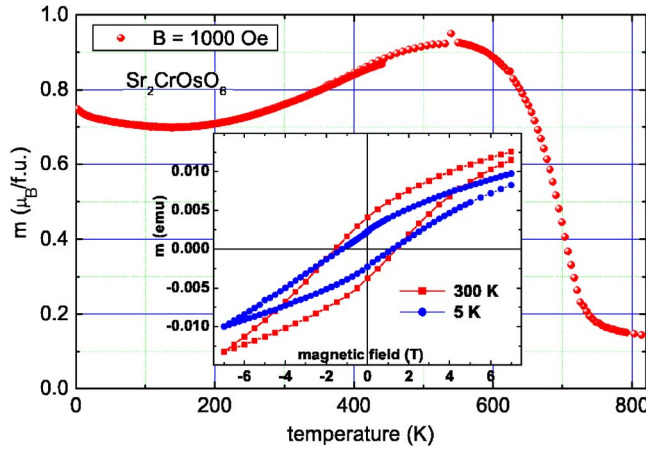


FIG. 2. (Color online) Magnetization vs temperature and hysteresis (at 5 K and 300 K) of Sr<sub>2</sub>CrOsO<sub>6</sub> (measured in a SQUID). The sample has been cooled and field oriented in diamagnetic LiNO<sub>3</sub> (melting point 480 K) because of the high anisotropy field.

into a corundum crucible. The crucible was placed in a quartz tube which was further evacuated and sealed under high vacuum. The quartz tube was heated at 1273 K for 2 days. The obtained product was further heated under oxygen flow at 673 K overnight to remove excess Os metal as an impurity. Extensive x-ray and neutron diffraction analysis confirms the high phase purity of the samples (see Fig. 1). The antisite disorder is negligible below 0.1%.

In Fig. 1 neutron powder diffraction data collected with the instrument E9 (Ge monochromator selecting the neutron wavelength  $\lambda=1.7971$  Å) at the reactor BER II of the Hahn-Meitner-Institut in Berlin is shown. The detailed refinement results are presented in Table I. From data refinement one can say that the crystal structure is clearly cubic above the magnetic transition temperature. At 550 K the crystal struc-

TABLE II. Measured and calculated [using the generalized gradient approximation including spin-orbit coupling (GGA+SO)] magnetic moments of Sr<sub>2</sub>CrOsO<sub>6</sub> in  $\mu_B$ /f.u. For a detailed discussion of the applied band-structure calculation see, e.g., Refs. 10 and 11. Note that the neutron measurements are total moments per site. Calculated number of *d* holes at Os: 4.83.

Method	Cr $m_S$	Cr $m_L$	Os $m_S$	Os $m_L$
XMCD (300 K)			-0.17	0.015
Neutrons (298 K)	1.92		-0.12	
Neutrons (2 K)	2.03		-0.73	
GGA+SO (0 K)	2.216	-0.024	-1.214	0.122

ture can still be refined by assuming a cubic structure. At 300 K the sample is already rhombohedral. The upper right inset of Fig. 1 shows the temperature evolution of the (444) diffraction peak in cubic notation. At low temperatures the splitting into two peaks [(404) and (0 0 12) in the hexagonal notation] with an observed intensity ratio of about 3 clearly evidences the rhombohedral structure. The tolerance factor at low temperatures is still close to 1 ( $\sim 0.992$ ).

Figure 2 shows the net magnetization and hysteresis behavior of Sr<sub>2</sub>CrOsO<sub>6</sub> as measured in a SQUID magnetometer.  $T_C$  is estimated to be about 725 K. The magnetization maximum at 550 K is a consequence of the different temperature evolution of the Cr magnetic moments and the induced moments at the Os site (see inset of Fig. 3). The drop of local magnetic spin moment at the Os site with increasing temperature is clearly not associated with a change of the insulating sample behavior. It is most likely that the unusual magnetic behavior is coupled to the distortion of the lattice, as can be motivated from Table I. In the same temperature range where the Os moment changes, the Os and Cr oxygen octahedra are markedly twisted against each other (see top view of the crystal structure in the inset of Fig. 1 and the combined plot of lattice distortion and magnetic moments versus temperature in the inset of Fig. 2). Alternatively, one could invoke a difficult-to-understand very strong ferromagnetic coupling between the Cr ions along the chain Cr-O-Os-O-Cr. However, the finite induced magnetic moment at the

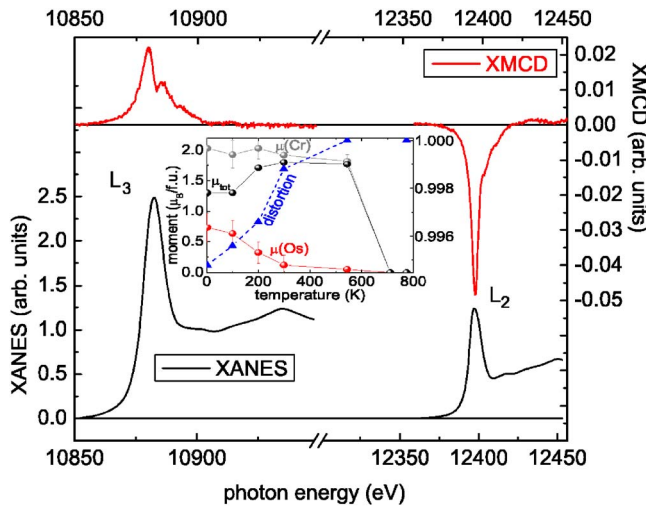


FIG. 3. (Color online) X-ray appearance near-edge structure (XANES) (left axis) and XMCD signal (right axis) at the Os  $L_2$  and  $L_3$  edges in Sr<sub>2</sub>CrOsO<sub>6</sub>. The inset shows the element-resolved magnetic moments of Cr ( $\mu_{Cr}$ ) and Os ( $\mu_{Os}$ ), the total magnetic moment ( $\mu_{tot}$ ), and the lattice distortion as determined from neutron scattering data refinement (see Table I).

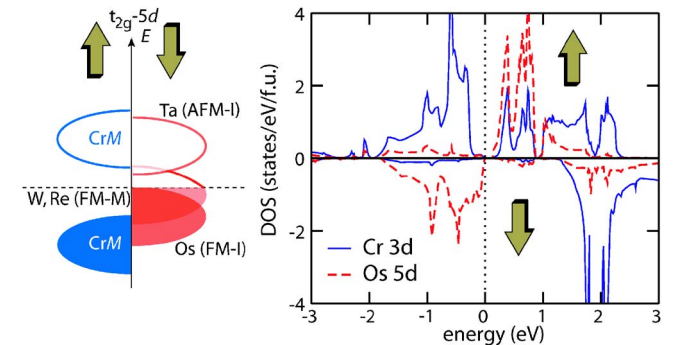


FIG. 4. (Color online) Left: band-structure sketch for different fillings of the 5*d* spin-down band (as realized in the materials Sr<sub>2</sub>CrMO<sub>6</sub> with  $M=Ta, W, Re, Os$ ). Right: band-structure calculation for Sr<sub>2</sub>CrOsO<sub>6</sub> using the generalized gradient approximation including spin-orbit coupling (GGA+SO).

Os site, although reduced to  $-0.05\mu_B$  at 540 K [for comparison, in  $\text{Sr}_2\text{FeReO}_6$  the total Re moment is only  $-0.16\mu_B$  at 5 K (Ref. 4)], survives up to  $T_C$ , indicating the validity of the kinetic energy gain model.

The XMCD measurements on the Os  $L_{2,3}$  edges were performed at the European Synchrotron Radiation Facility (ESRF) at beamline ID12.<sup>22</sup> As shown in Fig. 3 a very clear XMCD signal is observed, signaling a strong local magnetic moment at the Os site opposite to the net magnetization. The experimentally determined value is in good agreement with the neutron scattering result (see Table II).

Figure 4 (right side) shows the site-resolved density of states for the  $d$  states obtained from band-structure calculations in the experimentally observed low-temperature rhombohedral structure using the generalized gradient approximation (GGA) including spin-orbit coupling. The key result is that  $\text{Sr}_2\text{CrOsO}_6$  is, due to the completely filled Os  $t_{2g}$  spin-down orbitals, indeed at the end of spin-polarized metal-insulator transition (see sketch in Fig. 4, left side). This is also in agreement with conductivity measurements on the

powder samples, showing about  $10 \Omega \text{ cm}$  at room temperature. Our combined experimental and theoretical results show that the kinetic-energy-driven exchange mechanism<sup>6–8</sup> is not only operable in the itinerant range but in a wide range of conductivities.

In summary, we have unambiguously demonstrated that an increase of the number of  $5d$  electrons leads to an increase of the transition temperature in ferrimagnetic double perovskites irrespective of the changes in conductivity. Fully spin-polarized conductivity, as indicated by the large induced magnetic moments and supported further by band-structure calculations, can be changed from half-metallic behavior (known in  $\text{Sr}_2\text{CrWO}_6$  and  $\text{Sr}_2\text{CrReO}_6$ ) to insulating behavior in the high-Curie-temperature ferrimagnetic insulator  $\text{Sr}_2\text{CrOsO}_6$ .

The authors acknowledge support by the DFG (Project Nos. Al 560/4 and Ui 146/4), SSF, and VR. SNIC is acknowledged for providing computer facilities.

\*Electronic address: Y.Krockenberger@fkf.mpg.de

†Electronic address: alff@oxide.tu-darmstadt.de

<sup>1</sup>K.-I. Kobayashi, T. Kimura, H. Sawada, K. Terakura, and Y. Tokura, *Nature (London)* **395**, 677 (1998).

<sup>2</sup>J. B. Philipp, P. Majewski, L. Alff, A. Erb, R. Gross, T. Graf, M. S. Brandt, J. Simon, T. Walther, W. Mader, D. Topwal, and D. D. Sarma, *Phys. Rev. B* **68**, 144431 (2003).

<sup>3</sup>H. Kato, T. Okuda, Y. Okimoto, Y. Tomioka, Y. Takenoya, A. Ohkubo, M. Kawasaki, and Y. Tokura, *Appl. Phys. Lett.* **81**, 328 (2002).

<sup>4</sup>J. M. De Teresa, D. Serrate, C. Ritter, J. Blasco, M. R. Ibarra, L. Morellon, and W. Tokarz, *Phys. Rev. B* **71**, 092408 (2005).

<sup>5</sup>For a recent review see D. Serrate, J. M. De Teresa, and M. R. Ibarra, *J. Phys.: Condens. Matter* **19**, 023201 (2007).

<sup>6</sup>D. D. Sarma, P. Mahadevan, T. Saha-Dasgupta, S. Ray, and A. Kumar, *Phys. Rev. Lett.* **85**, 2549 (2000); see also *Curr. Opin. Solid State Mater. Sci.* **5**, 261 (2001).

<sup>7</sup>J. Kanamori and K. Terakura, *J. Phys. Soc. Jpn.* **70**, 1433 (2001).

<sup>8</sup>Z. Fang, K. Terakura, and J. Kanamori, *Phys. Rev. B* **63**, 180407(R) (2001).

<sup>9</sup>Horng-Tay Jeng and G. Y. Guo, *Phys. Rev. B* **67**, 094438 (2003).

<sup>10</sup>G. Vaitheeswaran, V. Kanchana, and A. Delin, *Appl. Phys. Lett.* **86**, 032513 (2005).

<sup>11</sup>G. Vaitheeswaran, V. Kanchana, and A. Delin, *J. Phys.: Conf. Ser.* **29**, 50 (2006).

<sup>12</sup>P. Majewski, S. Geprägs, O. Sanganas, M. Opel, R. Gross, F. Wilhelm, A. Rogalev, and L. Alff, *Appl. Phys. Lett.* **87**, 202503 (2005).

<sup>13</sup>P. Majewski, S. Geprägs, A. Boger, M. Opel, A. Erb, R. Gross, G. Vaitheeswaran, V. Kanchana, A. Delin, F. Wilhelm, A. Rogalev, and L. Alff, *Phys. Rev. B* **72**, 132402 (2005).

<sup>14</sup>M. Sikora, Cz. Kapusta, M. Borowiec, C. J. Oates, V. Prochazka, D. Rybicki, D. Zajac, J. M. De Teresa, C. Marquina, and M. R. Ibarra, *Appl. Phys. Lett.* **89**, 062509 (2006).

<sup>15</sup>M. Wojcik, E. Jedryka, S. Nadolski, D. Rubi, C. Frontera, J. Fontcuberta, B. Jurca, N. Dragoe, and P. Berthet, *Phys. Rev. B* **71**, 104410 (2005).

<sup>16</sup>J. Navarro, C. Frontera, Ll. Balcells, B. Martínez, and J. Fontcuberta, *Phys. Rev. B* **64**, 092411 (2001).

<sup>17</sup>C. Frontera, D. Rubi, J. Navarro, J. L. García-Muñoz, J. Fontcuberta, and C. Ritter, *Phys. Rev. B* **68**, 012412 (2003).

<sup>18</sup>J. B. Philipp, D. Reisinger, M. Schonecke, A. Marx, A. Erb, L. Alff, R. Gross, and J. Klein, *Appl. Phys. Lett.* **79**, 3654 (2002).

<sup>19</sup>S. Geprägs, P. Majewski, R. Gross, C. Ritter, and L. Alff, *J. Appl. Phys.* **99**, 08J102 (2006).

<sup>20</sup>L. Alff, in *Electron Correlation in New Materials and Nanosystems*, Vol. 241 of *NATO Advanced Study Institute, Series II*, edited by K. Scharnberg and S. Kruchinin (Springer, in press).

<sup>21</sup>A. W. Sleight, J. Longo, and R. Ward, *Inorg. Chem.* **1**, 245 (1962).

<sup>22</sup>A. Rogalev, J. Goulon, Ch. Goulon-Ginet, and C. Malgrange, in *Magnetism and Synchrotron Radiation*, edited by E. Beaurepaire *et al.*, *Lecture Notes in Physics*, Vol. 565 (Springer, Berlin, 2001).

<sup>23</sup>Y. Krockenberger, M. Reehuis, M. Tovar, K. Mogare, M. Jansen, and L. Alff, *J. Magn. Magn. Mater.* (to be published).